Title : Targeted delivery of flagellin by nebulization offers optimized respiratory immunity and defense against pneumococcal pneumonia

Author list

Mara Baldry[1*§], Charlotte Costa[1*], Yasmine Zeroual[1*], Delphine Cayet[1], Jeoffrey Pardessus[2,3], Daphnée Soulard[1], Frédéric Wallet[1], Delphine Beury[4], David Hot[4], Ronan MacLoughlin[5], Nathalie Heuzé-Vourc'h[2,3*], Jean-Claude Sirard[1*§], Christophe Carnoy[1*]

Affiliations

[1] Univ. Lille, CNRS, Inserm, CHU Lille, Institut Pasteur de Lille, U1019 - UMR 9017 - CIIL - Center for Infection and Immunity of Lille, F-59000 Lille, France

[2] INSERM, Respiratory Disease Research Centre, U1100, F-37032 Tours, France

[3] University of Tours, F-37032 Tours, France

[4]Univ. Lille, CNRS, Inserm, CHU Lille, Institut Pasteur de Lille, US 41 - UAR 2014 – PLBS - Plateformes Lilloises de Biologie & Santé, F-59000 Lille, France

[5]Aerogen, IDA Business Park, Dangan, Galway, Ireland

[*]Contributed equally

[§]Correspondence: mara.baldry@inserm.fr or jean-claude.sirard@inserm.fr

Abstract

Novel therapeutic strategies are urgently needed to combat pneumonia caused by *Streptococcus pneumoniae* strains resistant to standard-of-care antibiotics. Previous studies have shown that targeted stimulation of lung innate immune defenses through intranasal administration of the Toll-like receptor 5 agonist flagellin, improves the treatment of pneumonia when combined with antibiotics. To promote translation to the clinic application, this study assessed the direct delivery of flagellin to the airways through nebulization using a vibrating mesh nebulizer in mice. Intranasal delivery achieved approximately 40% lung deposition of the administered flagellin dose, whereas nebulization yielded less than 1%. Despite these differences, nebulized flagellin induced a transient activation of lung innate immunity characterized by cytokine/chemokine production and neutrophil infiltration into airways analogous to intranasal administration. Furthermore, inhalation by nebulization resulted in an accelerated resolution of systemic pro-inflammatory responses. Lastly, adjunct therapy combining nebulized flagellin and amoxicillin proved effective against antibiotic-resistant pneumococcal pneumonia in mice. We posit that flagellin aerosol therapy represents a safe and promising approach to address bacterial pneumonia within the context of antimicrobial resistance.

Keywords: Nebulization, intranasal, flagellin, pneumococcal pneumonia, deposition, inhalation, vibrating mesh nebulizer

42 **1. Introduction**

43 *Streptococcus pneumoniae*, commonly known as pneumococcus, typically inhabits the human
44 nasopharynx but can cause severe and often fatal diseases upon invasion of the host, such as
45 pneumonia [1]. While vaccines prevent pneumococcal pneumonia, they target only a fraction
46 of the nearly 100 serotypes identified thus far [2]. Consequently, there has been a rise in
47 infections caused by serotypes not included in the current available vaccines, many of which
48 exhibit antimicrobial resistance (AMR) [3, 4]. Resistance of *S. pneumoniae* to β-lactam
49 antibiotics such as amoxicillin (the standard of care for pneumococcal pneumonia) as well as
50 macrolides, is a major concern worldwide with the prevalence of resistance likely exceeding
51 20% in Europe alone [5]. Given the slow pace of new antimicrobial innovation and discovery
52 [6], it is imperative to explore alternative therapeutic strategies to treat pneumococcal
53 pneumonia otherwise untreatable with antibiotics.

54 Host-immune directed therapy, also referred to as immunotherapy, is a promising alternative
55 strategy to antibiotics aimed at either activating antimicrobial immunity or modulating
56 inflammation [7]. Toll-like receptors (TLRs) are pivotal pattern-recognition receptors involved
57 in orchestrating the antimicrobial immune defenses. TLRs can recognize pathogen-associated
58 or damage-associated molecular patterns and are widely expressed, particularly in immune
59 cells and structural cells [8]. TLR agonists have been developed as immunotherapeutic agents
60 in the field of infectious diseases. For example, the TLR5 agonist flagellin, a key structural
61 protein of the bacterial flagellum, demonstrates notable immunotherapeutic potential against
62 respiratory infections [9]. Flagellin is highly soluble and can be readily formulated in a saline
63 solution for delivery in human, including inhalation. TLR5 is expressed by airway epithelial
64 cells that are recognized as the principal drivers of TLR5-mediated protection. These cells
65 orchestrate the production of cytokines, chemokines, and antimicrobial peptides, and facilitate
66 the recruitment and activation of immune cells within the airways, particularly neutrophils [10-

67 12]. Inhalation of flagellin prior to infection was found protective against pneumonia caused
68 by *Streptococcus pneumoniae*, *Pseudomonas aeruginosa* and *Burkholderia cepacia* [12-14].
69 When combined with oral amoxicillin or intraperitoneal sulfamethoxazole, inhaled flagellin
70 demonstrates synergistic effects, leading to a substantial decrease in pneumococcal load within
71 the lungs of infected mice, otherwise not achieved with antibiotic or flagellin monotherapy [15,
72 16]. This combined treatment enables a reduction in the antibiotic dosage required to achieve
73 a comparable therapeutic outcome observed with antibiotic. More importantly, the synergistic
74 effect is also seen when the mice are infected with amoxicillin-resistant pneumococcus [15].
75 Additionally, adjunct flagellin therapy to antibiotics attenuates the selection of antibiotic
76 resistant strains in a co-infection model emphasizing the relevance of this approach in
77 combating AMR [17]. Another example of TLR agonist application in respiratory
78 immunotherapy was demonstrated by the exposure of mice to aerosolized TLR2/6 and TLR9
79 agonists, which induced protection to subsequent respiratory infections with viruses or bacteria
80 through the induction of respiratory innate immunity [18-21].
81 For treating infections of the lower respiratory tract, *i.e.,* pneumonia, direct delivery to the
82 lungs is obvious, matching the delivery route and the pathogen location. The method of
83 delivering therapeutics to the lungs depends on the clinical situation, the drug nature and its
84 formulation, and it is crucial to deliver a therapeutic dose of the drug to the target site [22-26]
85 While intranasal administration is a common method for targeting therapeutics into conducting
86 airway in animal studies, it is not adapted to target the lungs, in particular the deep lungs, in
87 humans [27]. Nebulization delivery, which produces an aerosol, stands out as the most efficient
88 approach for administering drugs and biologics as liquid forms, into the lungs in patients under
89 both spontaneous breathing and mechanical ventilation [23-25]. Vibrating mesh nebulizers
90 allow for fast, effective and user-friendly drug delivery to the airways [28-30]. Moreover, they
91 are usually more appropriate for biologics, limiting adverse effects during the aerosol

92 generation [24, 26, 31]. Adapting flagellin to aerosol delivery is an important step towards the
93 development of clinical investigations.
94 Here, we describe the use of a custom-made nebulization chamber for nose-only delivery of
95 aerosols in mice using a vibrating mesh nebulizer, and studied the fate and activity of nebulized
96 flagellin (hereafter referred to as FLAMOD), the activation of lung innate immunity, and the
97 therapeutic efficacy in combination with antibiotics against pneumococcal pneumonia.
98 Comparing with intranasal administration as a benchmark, our study reveals that nebulizer-
99 mediated delivery of FLAMOD demonstrates comparable or superior efficacy in promoting
100 lung immunity and protection, despite lower amounts being delivered to the lung. Moreover,
101 it induces a less pronounced and enduring impact on systemic pro-inflammatory responses.
102

103 **2. Materials and Methods**

104 *2.1 Bacterial strains*

105 *Streptococcus pneumoniae* serotype 1 (clinical isolate E1586) was obtained from the National
106 Reference Laboratory—Ministry of Health, Uruguay [12]. *Streptococcus pneumoniae* serotype
107 19F (clinical isolate LILPNEUHC 19F) was obtained from the University Hospital of Lille
108 (Frédéric Wallet, CHU Lille, France); it is a multidrug-resistant clinical isolate from a
109 bacteremia patient, and is resistant to amoxicillin (minimal inhibitory concentration, MIC_{AMX}
110 = 1.5 μg/ml), erythromycin and tetracycline, and has intermediate resistance to cefotaxime and
111 ceftriaxone. Working stocks were prepared as described previously [12]. Briefly, fresh colonies
112 grown on blood- agar plates were incubated in Todd Hewitt Yeast Broth (Sigma-Aldrich, Saint-
113 Louis, MO) at 37°C until the OD_{600nm} reached 0.7–0.9 units. Cultures were stored at −80°C
114 in broth + glycerol 12% (vol./vol.) for up to 3 months. For infection, working stocks were
115 thawed and washed with sterile Dulbecco's Phosphate-Buffered Saline (PBS, Gibco, Grand
116 Island, NY) and diluted to the appropriate concentration. The number of bacteria (as colony
117 forming units [CFUs]) was confirmed by plating serial dilutions onto 5% sheep blood agar
118 plates and incubating at 37°C for 18 h with 5% CO_2.

119

120 *2.2 FLAMOD preparation*

121 Flagellin was produced in *Escherichia coli* by the Vaccine Development department at Statens
122 Serum Institut, Denmark. The custom-designed flagellin used in the present study, *i.e.,*
123 FLAMOD (recombinant flagellin $FliC_{\Delta 174\text{-}400}$ as described in Nempont et al 2008 [32]
124 harboring one extra amino acid at the N terminus) derives from *Salmonella enterica* serovar
125 Typhimurium FliC. FLAMOD was purified by filtration and chromatography and resuspended
126 in NaPi buffer: 10 mM phosphate, 145 mM NaCl, polysorbate 80 0.02 % (w/v) pH 6.5.
127 Immunostimulatory activity was validated using the HEK-Dual™ hTLR5 cells assay

128 (Invivogen). The endotoxin content in the protein preparation was assessed with
129 a *Limulus* assay (Pyrochrome, kinetic LAL assay from Associates of Cape Cod Inc.).
130
131 *2.3 Mouse treatment and infection*
132 All experiments complied with institutional regulations and ethical guidelines, were approved
133 by Institutional Animal Care and Use Committee (E59-350009, Institut Pasteur de Lille;
134 Protocol APAFIS#16966 201805311410769_v3) and were conducted by qualified personnel.
135 Female BALB/cJRj mice, male C57BL/6JRj mice (6–8 weeks old) (Janvier Laboratories, Saint
136 Berthevin, France) and female and male *Tlr5*$^{-/-}$ (varying ages, breed in-house on C57BL/6JRj
137 background) were maintained in ventilated cages (Innorack® IVC Mouse 3.5) and handled in
138 a laminar flow biosafety cabinet (Class II Biohazard, Tecniplast).
139 Intranasal treatment was performed with 2.5 µg or 30 µg FLAMOD in 30 µl NaPi buffer that
140 was administered intranasally under light anesthesia via isoflurane inhalation (Axience, Pantin,
141 France). The dose of 2.5 µg of FLAMOD has been previously demonstrated protective in
142 pneumococcal infections while the dose of 30 µg corresponds to the amount of FLAMOD used
143 for the biodistribution analysis. Control animals (mock treated) received intranasal NaPi buffer
144 alone. For FLAMOD administration using the Aerogen® Solo vibrating mesh nebulizer
145 (Aerogen, Ireland) in combination with ProX controller (Aerogen, Ireland), a custom-made
146 chamber was used (EuroBioConcept, Bonneuil sur Marne, France). One milliliter of NaPi
147 buffer or FLAMOD at 250 µg/mL was administered for 4-5 minutes to vigilant mice using the
148 Aerogen® Solo nebulizer (**Supplementary Figure 1**). For intravenous administration,
149 FLAMOD was injected retro-orbitally at concentrations of 10 or 30 µg per mouse prepared in
150 200 µl PBS. After treatment, mice were sacrificed via the intraperitoneal injection of 5.47 mg
151 sodium pentobarbital in 100 µl PBS. Broncholalveolar lavage (BAL) fluids were obtained by
152 intratracheal injection of 2 × 1 ml PBS supplemented with protease inhibitors (Roche). Serum

153 was collected by intracardiac puncture and separated from whole blood in Z-Gel microtubes
154 (Sarstedt). BAL and serum samples were stored at −20°C prior to analysis.
155 Prior to infection, the mice were anesthetized via the intraperitoneal injection of 1.25 mg (50
156 mg/kg) ketamine plus 0.25 mg (10 mg/kg) xylazine in 250 µl of PBS. For primary infections
157 with the serotype 1 isolate E1586 in BALB/c mice, $2x10^6$ CFU were inoculated intranasally in
158 30 µl PBS, as described previously [16]. For the pneumococcal superinfection, C57BL/6 mice
159 were used as previously described [16, 33]. In this model, animals were first infected i.n.with
160 50 plaque-forming units (PFU) of the pathogenic, murine-adapted H3N2 influenza A virus
161 strain Scotland/20/74 in 30 µl of PBS. Seven days later, i.n. *S. pneumoniae* infection was
162 induced with $1x10^5$ CFU of the serotype 19F strain in 30 µl of PBS. Mice were treated 12 h
163 post-infection with intranasal or nebulized FLAMOD and with intragastric administration of 5
164 µg or 1 mg of amoxicillin (Clamoxyl for injection, GlaxoSmithKline) in 200 µl of water. Mock
165 treated control animals received NaPi buffer and water. After 24 h infection, lungs and spleen
166 were homogenized with an UltraTurrax homogenizer (IKA-Werke, Staufen, Germany), and
167 viable bacterial counts were determined on blood agar plates.
168
169 *2.4 FLAMOD-specific ELISA*
170 Maxisorp 96 well (Nunc 442404) plates were coated with 50 µl of capture anti-FLAMOD
171 monoclonal antibody (Mab, 9H10-R2-2E8 mouse IgG1 - lot vt220802-7034) at 5µg/ml in D-
172 PBS 1X (PBS, Gibco 14190-094) and incubated overnight at 4°C. The plates were washed 3
173 times with PBS/Tween 20 0.05% (PBS-T) and saturated for 2 h at room temperature (RT) with
174 300 µl per well ELISA/ELISPOT diluent 1X (Invitrogen 00-4202-56, 5X solution diluted in
175 sterile water Versylene Fresenius B230531). The plates were washed again 3 times with
176 PBS/T. Serum samples were diluted 1:5 in ELISA /ELISPOT diluent (i.e., 20% final ratio of
177 mouse serum), BAL samples 1:200 and 50 µl were distributed per well in the microplates. To

178 generate a calibration curve, FLAMOD (lot 4182.5) was diluted from 100 ng/ml to 0.78 ng/ in
179 ELISA /ELISPOT diluent substituted with 20% mouse serum (in-house serum harvested from
180 naïve C57BL/6JRj mice) and 50 µl were distributed per well. Plates were incubated for 2 h at
181 RT and washed 3 times with PBS-T. Fifty µl per well of the biotinylated FLAMOD-specific
182 detection Mab (4C1H7 mouse IgG1 - lot b220809-7034, [34]) diluted at 2 µg/ml in
183 ELISA/ELISPOT diluent were distributed and incubated for 1 h at RT. Plates were washed 3
184 times with PBS-T and 50 µl per well of the avidin-HRP (eBioscience 18-4100-51) diluted
185 1:2000 in ELISA/ELISPOT diluent were added and incubated for 25 min at RT. Plates were
186 washed 5 times with PBS-T. The reaction was developed using 50 µl per well of the TMB
187 substrate reagent (Interchim ref: UP664781). Plates were incubated for 5 min at RT in the dark,
188 prior to stopping the reaction by adding 25 µl H_2SO_4 2N per well. The plates were read
189 immediately at 450 nm absorbance and subtracted at 540-570 nm. The values were transformed
190 using a four-parameter logistic regression (R^2>0.99) to calculate the concentration of
191 FLAMOD in the biological samples.
192
193 *2.5 Transcriptional analysis by RT-qPCR and RNA sequencing*
194 Total RNA was extracted with the Nucleospin RNA Plus kit (Macherey Nagel, Düren,
195 Germany). Trachea and whole lungs were homogenized in RA1 buffer with an UltraTurrax
196 homogenizer. Lysates of nasal cavity were obtained by injecting 500 µl RA1 buffer through a
197 22-gauge canula that was inserted into the posterior naris along the direction of the nostrils and
198 collecting from the anterior naris. Bronchial epithelium sampling was performed as described
199 [35]. Briefly, sanded PE50 tubing was inserted into the main bronchus via the trachea with
200 gentle brushing and immediately processed for RNA extraction. Total RNA was reverse-
201 transcribed with the High-Capacity cDNA Archive Kit (Applied Biosystems, Foster City, CA).
202 The cDNA was amplified using SYBR green- based real-time PCR on a Quantstudio 12K PCR

203 system (Applied Biosystems). Relative mRNA levels ($2^{-\Delta\Delta Cq}$) were determined by
204 comparing first the PCR cycle thresholds (Cq) for the gene of interest and the reference genes
205 *Actb* and *B2m* (ΔCq), and then the ΔCq values for treated vs. control group ($\Delta\Delta Cq$). All the
206 primers used in this study are listed in **Supplementary Table 1**.
207 For sequencing, RNA concentration and quality were evaluated by spectrophotometry
208 (Nanodrop) and the TapeStation 4200 (Agilent Technologies), respectively. The libraries were
209 prepared using the QIAseq stranded mRNA library kit (Qiagen), quantified by quantitative
210 PCR (KAPA Library Quantification Kit for Illumina platforms; KapaBiosystems) and pooled
211 in an equimolar manner prior to sequencing on a NovaSeq sequencer (Illumina) in 2 × 150 bp.
212 RNA sequencing data (FASTQ files) were mapped to the mouse genome build (GRCm39)
213 with STAR (STAR-2.7.10a). The mapped reads were annotated using GENCODE M30 GTF
214 file. Differentially expressed genes analysis (DEG) were performed using the DESeq2 package
215 (1.38.2 [36]). Median of ratio method was used for data normalization. Genes with null sum of
216 read counts were filtered out. Genes with p-adjusted value < 0.05 and log2 fold change >1 were
217 considered as differentially expressed. Over-Representation Analysis (ORA) was performed
218 using ClusterProfiler (version 4.6.2) and the functions enrichGo and CompareCluster to
219 identify Biological Processes. Analysis was carried out using Bioconductor (version 3.16.0).
220 Sequencing data have been deposited in the National Center for Biotechnology Information's
221 Gene Expression Omnibus repository under the accession number GSE252037.
222
223 *2.6 Cytokine and chemokine production*
224 Protein concentrations of CCL20, CXCL2, IL-6, IL-22, and SAA were determined in BAL
225 fluids and serum by enzyme- linked immunosorbent assay (ELISA kit from eBioscience, R&D
226 Systems or Becton Dickinson).
227

228 *2.7 Scintigraphy in mice*

229 All scintigraphy experiments were conducted on male C57BL/6JRj (9-16 weeks old), approved
230 by local ethics committee and recorded under the agreement reference N°11682-
231 201700217166146. Prior to the scintigraphy study, a perfusion scintigraphy study was
232 performed to evaluate technetium 99m (^{99m}Tc) γ-rays absorption by tissues. Mice were slightly
233 sedated via isoflurane inhalation (Vetflurane, Virbac, France) and a suspension of macro
234 aggregates labeled with ^{99m}Tc (^{99m}Tc-MAA, Pulmocis, Curium Pharma, France) was
235 intravenously injected through the tail vein. After ensuring that all ^{99m}Tc-MAA was trapped in
236 the pulmonary capillaries, animals were imaged in anterior static position using Biospace®
237 gamma imager (Biospace, France) for 60 seconds under isoflurane anesthesia. This step
238 allowed to determine the attenuation coefficient of animal tissues against γ-rays, which must
239 be considered when calculating activity measured in mice, and takes into account the
240 background activity and radioactive decay of technetium. Moreover, it allows the illustration
241 of the region of interest (ROI). For the scintigraphy study, inhalation by intranasal and
242 nebulization routes were compared. For intranasal delivery mice were sedated, then 40 µL of
243 0.9% NaCl solution mixed with diethylenetriaminepentaacetic acid labeled with ^{99m}Tc (^{99m}TC-
244 DTPA, Technescan™ DTPA, Curium Pharma, France) were rapidly administered. For the
245 nebulization route, experiments were performed as described in 2.3 using the custom-made
246 nebulization chamber and an Aerogen® Solo to nebulize 1 mL of 0.9% NaCl solution mixed
247 with 0.1 mL of ^{99m}TC-DTPA (n=4 per nebulization round). Immediately after i.n. or nebulized
248 administration, mice were imaged for 120 seconds under isoflurane anesthesia.

249

250 *2.8 Histology and staining*

251 The left lung from each mouse was collected in buffered 10% formalin (Q-Path VWR
252 Chemicals), included in paraffin, and 3- to 5-µm tissue sections were prepared (Althisia,

253 Troyes, France). Tissue sections (n=3 for FLAMOD treated and n=2 for untreated control)
254 were stained with a classical hematoxylin and eosin reagent or processed for
255 immunohistochemistry. Immunohistochemistry on neutrophils was performed using rabbit
256 monoclonal anti-Ly6G antibody (clone EPR22909-135). The Ly6G-stained images were
257 evaluated for neutrophil infiltration.

258

259 *2.9 Statistical Analysis*

260 Results were expressed as individual values and median [interquartile range] or mean ±
261 standard error of the mean (SEM). Groups were compared using a Kruskal-Wallis one-way
262 analysis of variance (ANOVA) with Dunn's post-test (for three or more groups) and two-way
263 ANOVA mixed model with Šídák's multiple comparisons test. All analyses were performed
264 using GraphPad Prism software (version 10.10, GraphPad Software Inc., San Diego, CA), and
265 the threshold for statistical significance was set to $p<0.05$.

266

267 **3. Results**

268

269 *3.1 Fate of inhaled FLAMOD in mice after intranasal and aerosol administration*

270 Understanding the fate of inhaled flagellin is imperative to characterizing its safety and efficacy
271 parameters as an adjunct to antibiotics. The outcome of flagellin (defined here as FLAMOD)
272 was investigated after intranasal administration of 30 µg FLAMOD in bronchoalveolar lavages
273 (BAL), as a surrogate of lung deposition, and serum using a FLAMOD-specific ELISA.
274 Immediate recovery after administration (<5 min) revealed that around 30 % of the
275 administered FLAMOD reached the lungs, *i.e.,* 8.6 ± 2.0 µg (**Figure 1A**). Similar levels of
276 lung deposition (~45 %) were defined using scintigraphy (**Figure 1C-D).** FLAMOD was
277 rapidly degraded over time and became undetectable after 24 h. In addition, serum levels of
278 FLAMOD remained consistently below the lower limit of quantification (LLOQ), *i.e.,*
279 <4 ng/mL, at all timepoints following administration.

280 Mice were also exposed to nebulized FLAMOD (1 ml at 250 µg/mL) for 5 min using a
281 customized chamber connected to an Aerogen® Solo mesh nebulizer
282 (**Supplementary Figure 1A-B**). FLAMOD deposition in BAL reached 25 ± 16 ng
283 immediately after aerosolization and decreased to below the LLOQ within the first 2 h
284 (**Figure 1B**). In contrast, scintigraphy determined that 0.52 % lung deposition after
285 nebulization is achieved which is equivalent to 1.30 µg FLAMOD (**Figure 1E-F**). FLAMOD
286 was undetectable in serum post-nebulization, indicating no systemic leakage. The difference
287 in lung deposition between the two analytical methods (ELISA and scintigraphy) highlights
288 differing sensitivities and suggests rapid degradation of FLAMOD upon aerosol delivery. To
289 better understand the fate of FLAMOD when in the circulatory compartment and to have a
290 positive reference for immune activation when FLAMOD is found directly in the systemic
291 compartment, FLAMOD was injected intravenously (**Supplementary Figure 2**). Serum levels

292 of FLAMOD corresponding to around 60% delivered dose were detected immediately after
293 injection (< 5 min) followed by a decline to <1% by 60 min post-administration. This suggests
294 rapid FLAMOD clearance. In conclusion, inhalation of FLAMOD by the intranasal or
295 nebulization route in mice provides local delivery without systemic leakage, while resulting in
296 distinct levels of lung deposition.
297

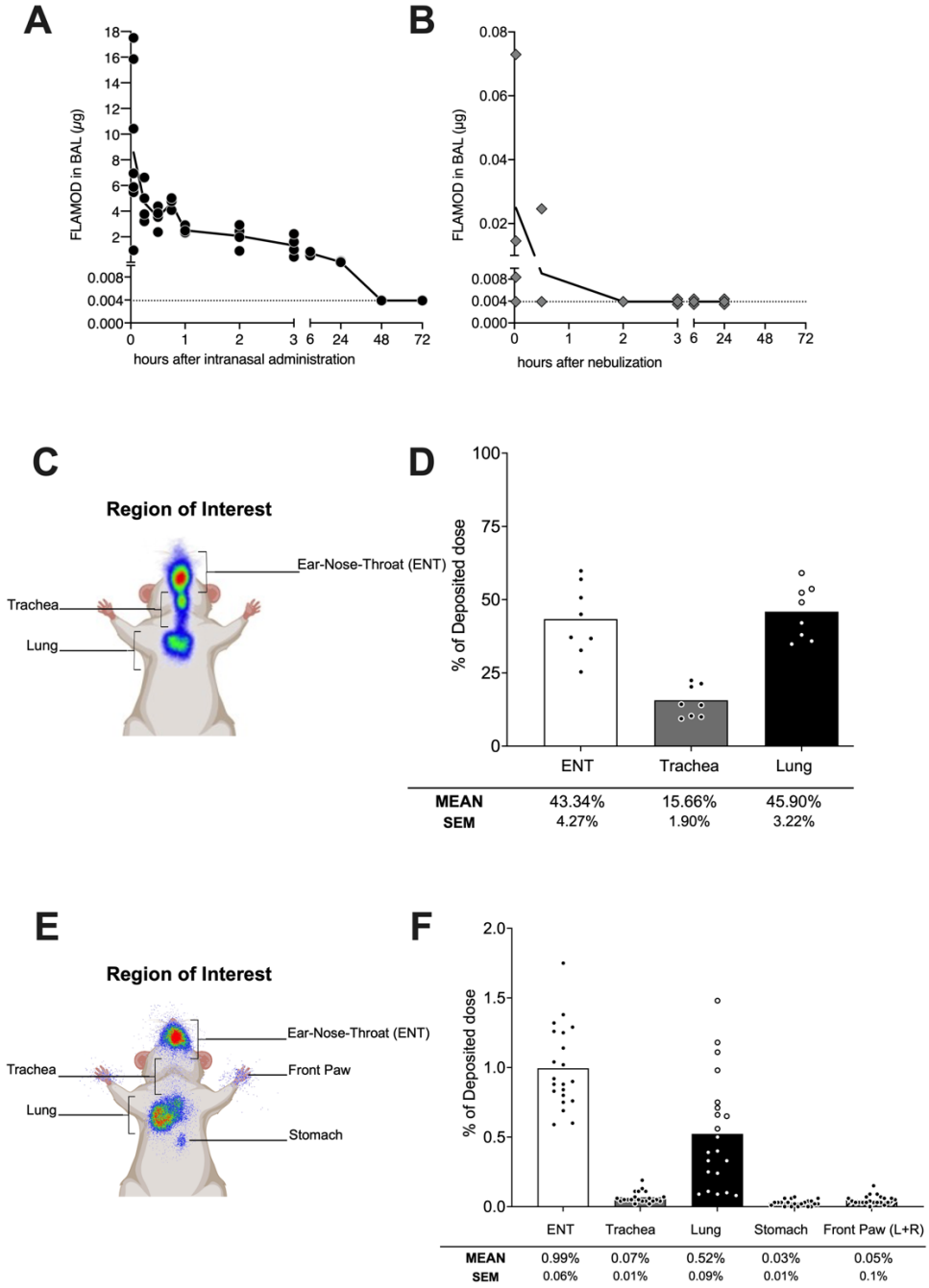

298

299 **Figure 1. FLAMOD biodistribution after intranasal or aerosol inhalation**. BALB/c mice
300 (n=4-8) per time point and treatment group) were subjected to intranasal administration of 30
301 µg FLAMOD or nebulization with 1 ml of FLAMOD at 250 µg/ml in NaPi buffer, utilizing a
302 mesh-nebulizer and aerosol chamber setup. Control groups were either treated with NaPi buffer
303 or left untreated. BAL was collected at varying timepoints to measure FLAMOD. **(A-B)**
304 FLAMOD deposition in BAL after **(A)** intranasal administration or **(B)** nebulization was
305 quantified using a FLAMOD-specific ELISA. Dotted line indicates LLOQ of FLAMOD, i.e.,
306 3.9 ng/ml. Deposition of intranasal FLAMOD (**C-D**) and nebulized FLAMOD (**E-F**) was
307 further analyzed by scintigraphy. Mice were subjected to intranasal administration of 0.9%
308 NaCl containing ^{99m}TC-DTPA (n=8), or nebulization with 0.9% NaCl containing ^{99m}TC-DTPA
309 (n=21). Left images show the regions of interest (ROI) where radioactivity was measured, and
310 the quantitative data for each ROI are presented on the right panel. The amount of aerosol
311 deposited is expressed as a percentage of the total amount administered.
312
313 *3.2 Immunostimulatory activity of inhaled FLAMOD*
314 We first confirmed the TLR5-dependent activation of immune mediators by FLAMOD using
315 TLR5 knock-out mice. As expected, when FLAMOD was provided intravenously to wild-type
316 and TLR5 knock-out mice respectively, no immune mediators (namely CCL20, IL-6 and IL-
317 22) were produced in the TLR5 knock-out mice in response to FLAMOD treatment
318 (**Supplementary Figure 3**). We next analyzed the TLR5-specific immune responses to
319 nebulized FLAMOD based on the expected immune outcomes after intranasal delivery [11, 32,
320 37-39]. The activation of respiratory innate immunity subsequent to intranasal or nebulization
321 delivery of FLAMOD exhibited comparable levels of CCL20, CXCL2 and IL-6 in BAL
322 (**Figure 2A**). However, aerosol delivery resulted in a less persistent immune response
323 compared to intranasal administration, generally returning to steady-state within a shorter

period to that of intranasal. Serum analysis revealed that nebulization triggered similar levels of IL-6 and CCL20, as well as shorter responses compared to intranasal delivery (**Figure 2B**). The serum concentration of the acute phase inflammation marker serum amyloid A (SAA) was globally lower in response to nebulization than intranasal delivery. Importantly, IL-22 was undetectable in serum after nebulization in contrast to intranasal route. We previously showed that IL-22 is produced when flagellin is found systemically but not when it stays in the mucosal compartment [39]. Thus, this cytokine indicates leakage of flagellin into the bloodstream and thus represents a surrogate marker of lung barrier integrity. The absence of IL-22 in the serum of nebulized mice suggests that FLAMOD does not cross the pulmonary barrier after nebulization, particularly when compared to the very high IL-22 levels detected in mice receiving FLAMOD intravenously (**Supplementary Figure 2**). These findings fully corroborate the data on FLAMOD biodistribution presented above.

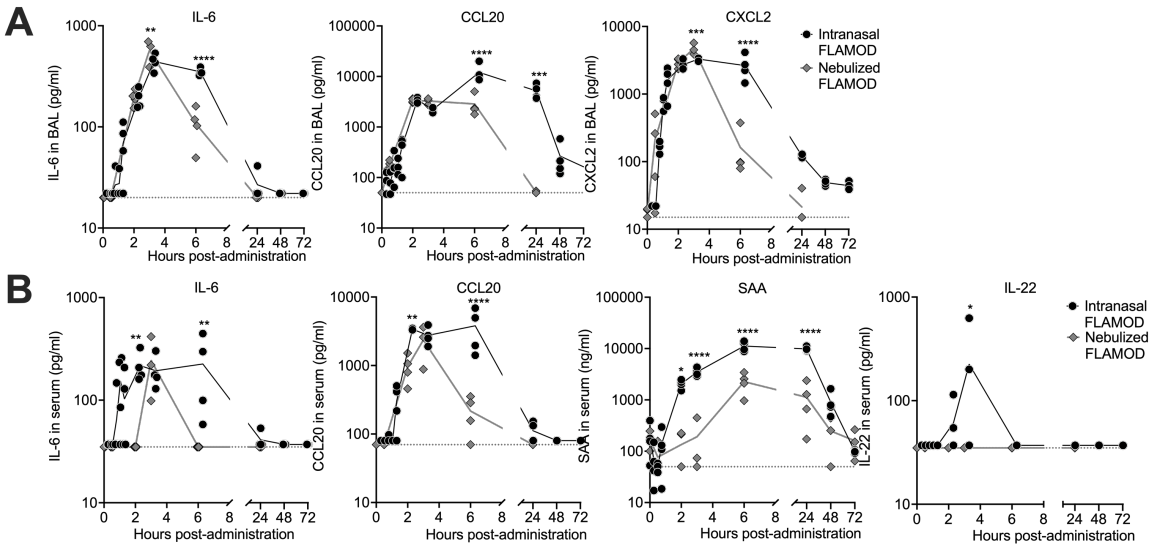

Figure 2. Transient innate immune activation following FLAMOD inhalation. BALB/c mice (n=4 per time point and treatment group) were subjected to intranasal administration of 30 µg FLAMOD or nebulization with 1 ml of FLAMOD at 250 µg/ml in NaPi buffer, utilizing a mesh-nebulizer and aerosol chamber setup, or left untreated. BAL and serum were collected at varying timepoints to monitor immune response. Cytokine and chemokine concentrations in

342 BAL fluids **(A)** and serum **(B)**. Dotted lines indicate LLOQ. Statistical differences were
343 analyzed using two-way ANOVA (*p<0.05, **p<0.01, ***p<0.001, ****p<0.0001).
344
345 Consistent with the findings from ELISA analysis of BAL (**Figure 1**) and similarly to the
346 previous finding following intranasal delivery [11, 32, 37], nebulized FLAMOD elicited a
347 temporary increase in transcriptional activity of pro-inflammatory genes, reaching its peak at
348 2 h post-administration (**Supplementary Figure 4)**. Given that inhalation delivers the drug
349 into the nose, trachea, bronchi and lung, we compared the gene expression from these
350 compartments 2 h after the treatment of animals with nebulized or intranasal FLAMOD and
351 normalized the expression profiles to the buffer treated animals (**Figure 3**). Inhaled FLAMOD
352 stimulated the transcription of *Il6*, *Ccl20* and *Cxcl2* in all respiratory compartments.
353 Interestingly, with the exception of the nasal compartment, activation levels were significantly
354 higher under the nebulization condition than for intranasal inhalation. This finding is also
355 intriguing when considering that scintigraphy data displayed negligible tracheal deposition
356 during nebulization (0.07%) as opposed to that deposited intranasally (15.7%), amounting to a
357 224-fold difference. To further compare the modes of inhalation, RNA-seq analysis was
358 conducted on lungs collected at 2 h after FLAMOD or buffer administration (**Figure 4 and**
359 **Supplementary Table 2**). This analysis identified 955 and 1470 differentially expressed genes
360 (DEG) that were significantly regulated ($\log_2 FC \geq 1$ and $p \leq 0.05$) by aerosol and intranasal
361 inhalation, respectively. Similar genes were up- and down-regulated for both types of
362 FLAMOD administration as depicted in **Figure 4A-B and Supplementary Table 2**. For both
363 inhalation modes, over-representation analysis (ORA) revealed a significant modulation of
364 signaling pathways associated with response to bacterial molecules, innate immunity and
365 innate receptors, NF-κB, cytokine/chemokine production, immune cell activation and
366 migration, defense to pathogens or negative regulation to dampen inflammation (**Figure 4C**

367 **and Supplementary Table 3**). Despite the significant disparity in FLAMOD deposition
368 observed across nebulization and intranasal delivery, our findings demonstrated that
369 nebulization is a potent method for eliciting TLR5-specific innate immune responses within
370 the respiratory tract.

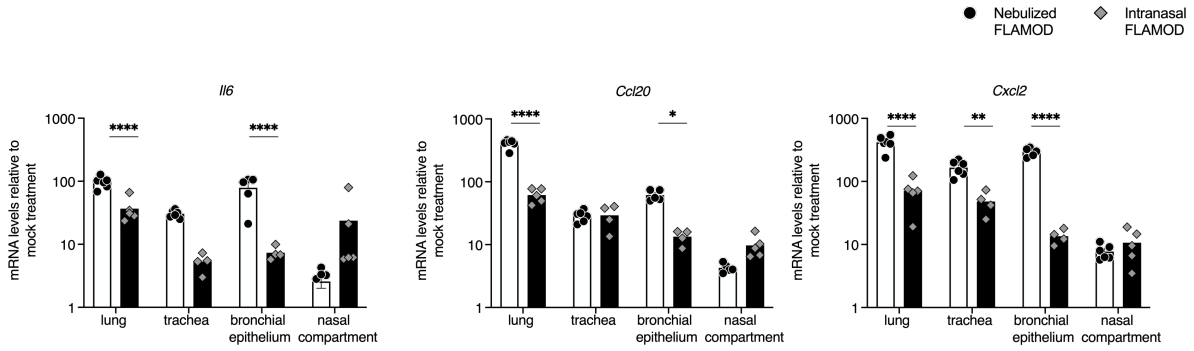

371

372 **Figure 3. Compartmentalization of transcriptional response to FLAMOD inhalation**.
373 BALB/c mice (n=5-6 per time point and treatment group) were subjected to intranasal
374 administration of 30 µg FLAMOD or nebulization with 1 ml of FLAMOD at 250 µg/ml in
375 NaPi buffer, utilizing a mesh-nebulizer and aerosol chamber setup, or mock treatment with
376 NaPi buffer. Lungs, trachea, bronchial epithelium and nasal lavages were analyzed at 2 h post-
377 administration**.** Gene expression of innate immune markers was measured by RT-qPCR. The
378 relative mRNA levels of selected genes are expressed against the reference gene *Actb* and
379 normalized to the mock condition. Statistical differences were analyzed using two-way
380 ANOVA (*$p<0.05$, **$p<0.01$, ****$p<0.0001$).

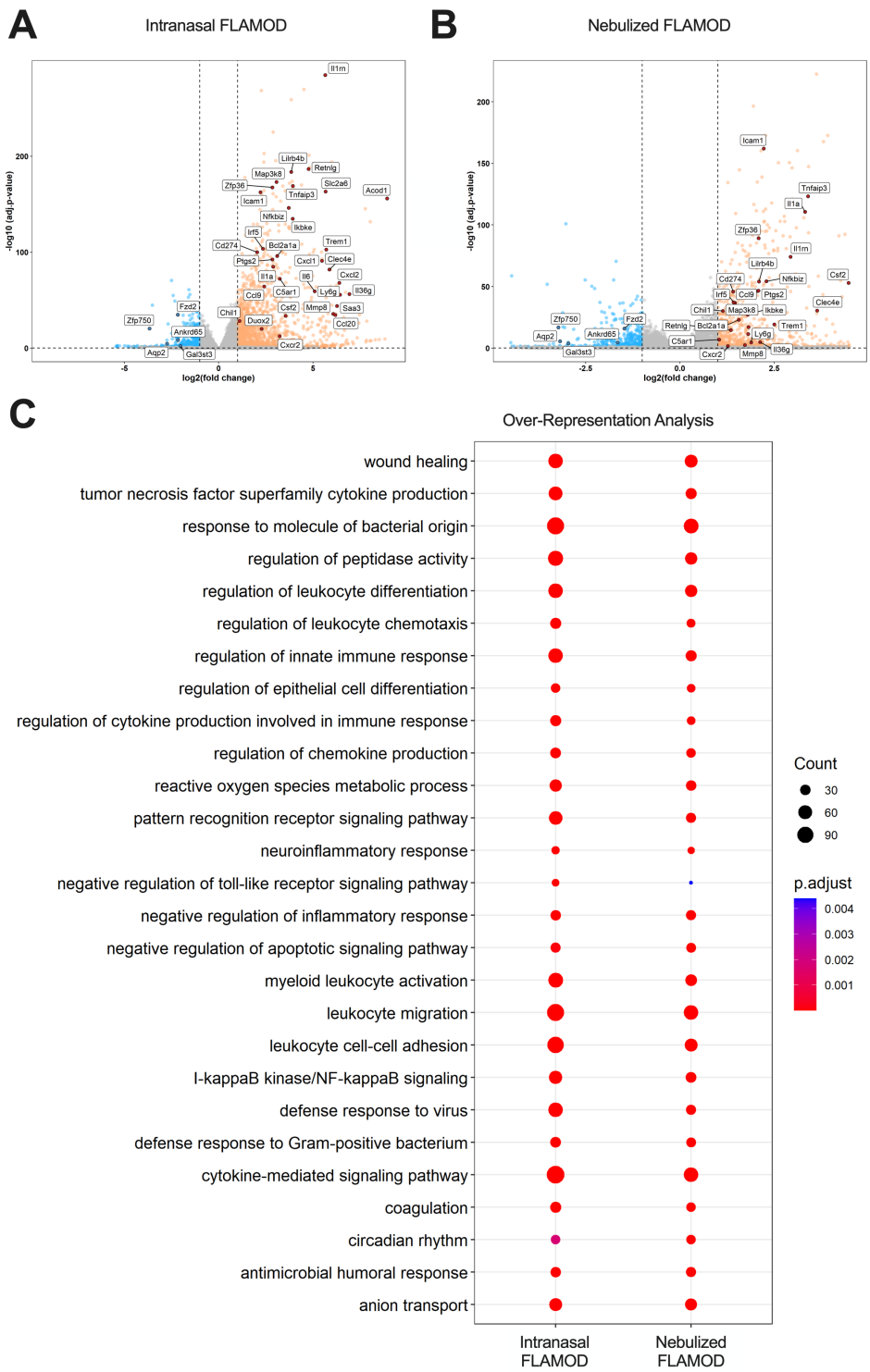

Figure 4. FLAMOD inhalation by the intranasal or nebulization route activates similar innate immune responses. BALB/c mice (n=4 per time point and treatment group) were subjected to intranasal administration of 30 µg FLAMOD or nebulization with 1 ml of FLAMOD at 250 µg/ml in NaPi buffer, utilizing a mesh-nebulizer and aerosol chamber setup,

386 or mock treatment with NaPi buffer. Lungs were collected 2 h post-administration for RNA
387 sequencing. **(A-B)** Volcano plots of DEG between intranasal FLAMOD and intranasal buffer
388 group **(A)** and nebulized FLAMOD and nebulized buffer group **(B)**. Labelled genes represent
389 the top DEG. **(C)** Immune pathways in nebulized and intranasal groups were identified using
390 ORA. The common biological processes enriched in both conditions are represented. The count
391 and p.adjust scales indicate the number of genes enriched in the pathway and the significance
392 of enrichment, respectively.
393
394 Neutrophil recruitment stands as a pivotal indicator of TLR5 activation within pulmonary
395 tissues [10, 16, 37, 40, 41]. To elucidate the influence of inhalation on this process, lung
396 samples were analyzed by immunohistochemical staining employing the anti-Ly6G antibody
397 for neutrophil detection (**Figure 5**). Evaluations were performed at two distinct time points: 4
398 hours post-treatment, coinciding with the peak of neutrophil recruitment in response to flagellin
399 [10, 37], and 24 hours post-treatment, representing a period wherein FLAMOD becomes
400 undetectable and most activation markers return to baseline levels. After 4 h, a comparable
401 pattern of neutrophil infiltration was observed between the two inhalation methods, with a
402 tendency for more clustering around the bronchioles rather than within the alveolar space.
403 However, a notable contrast emerged at 24 h between the intranasal and nebulized conditions.
404 In the intranasal group neutrophil presence remained elevated, while in the nebulized group the
405 level of infiltration resembled that of untreated controls. Taken together, these observations
406 suggest that nebulized FLAMOD can induce transient lung neutrophil infiltration, with a more
407 rapid return to baseline compared to intranasal administration.

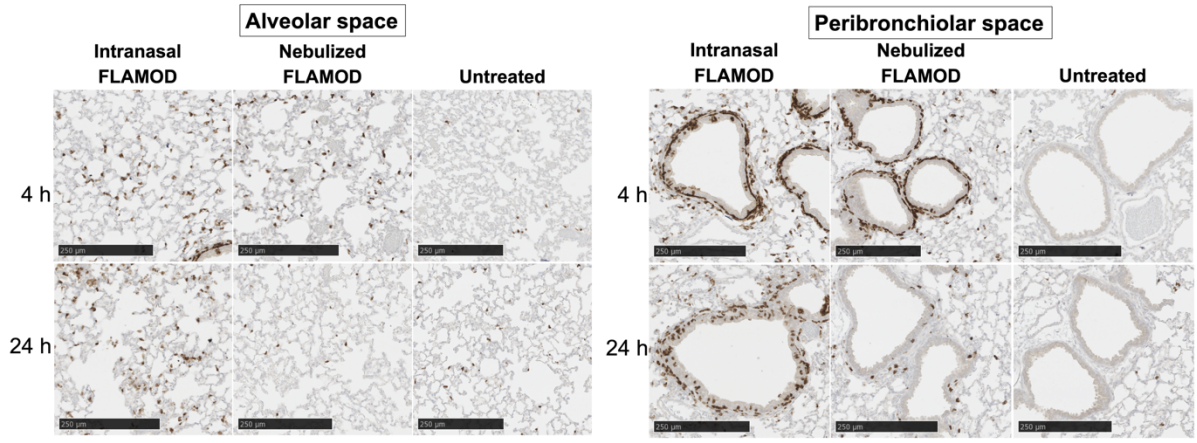

Figure 5. Transient neutrophil recruitment in response to FLAMOD inhalation. BALB/c mice (n=3 per FLAMOD treatment) were subjected to intranasal administration of 30 µg FLAMOD or nebulization with 1 ml of FLAMOD at 250 µg/ml in NaPi buffer, utilizing a mesh-nebulizer and aerosol chamber setup, or mock treatment with buffer (n=2). Lungs were collected 4 h and 24 h after FLAMOD inhalation and processed for immunohistochemical Ly6G-staining of neutrophils (brown). (**A**) Alveolar space and **(B)** peribronchiolar space. The images are representative of individual animals.

3.3 Therapeutic efficacy of nebulized FLAMOD against pneumococcal pneumonia

Nebulization of FLAMOD was next compared to intranasal delivery of FLAMOD as an adjunct therapy to the antibiotic amoxicillin (AMX) in a pneumococcal superinfection model (**Figure 6A**). To this end, the animals were superinfected with a serotype 19F of *S. pneumoniae* that displays resistance to AMX (MIC_{AMX}, of 1.5 µg/ml). As expected, treatment with AMX and intranasal FLAMOD substantially improved bacterial clearance compared to AMX alone (**Figure 6B**). The same synergy and efficacy were found when FLAMOD was nebulized resulting in significant reduction of bacterial burden in the lung as well as bacterial dissemination in spleen (**Figure 6C**). In the context of superinfection, the fate of FLAMOD in the BAL after intranasal inhalation or nebulization was in line with that observed for naïve mice (**Figure 6D-E**). However, FLAMOD was found at very low levels in the bloodstream of

428 mice treated intranasally, suggesting marginal leakage (**Figure 6D)**. The immune activation
429 profiles in lung and bloodstream were also similar to those seen in mice without prior infection,
430 implying that activity of inhaled FLAMOD did not change in the context of infection
431 (**Figure 6F-G**). Importantly, IL-22 was not detected in the bloodstream after nebulization with
432 FLAMOD, indicating that even when the lungs are compromised by infection, leakage is not
433 observed. Finally, the therapeutic synergy of nebulized FLAMOD with AMX was also
434 effective in a primary respiratory infection with a serotype 1 amoxicillin-sensitive strain
435 (MIC_{AMX} = 0.016μg/ml) (**Supplementary Figure 5**). Collectively, these data indicate that
436 despite the low lung deposition upon nebulization in mouse models of antibiotic-resistant and
437 antibiotic-sensitive pneumococcal infections, the delivered dose is sufficient to provide
438 therapeutic efficacy within the range observed for intranasal administration.

Figure 6

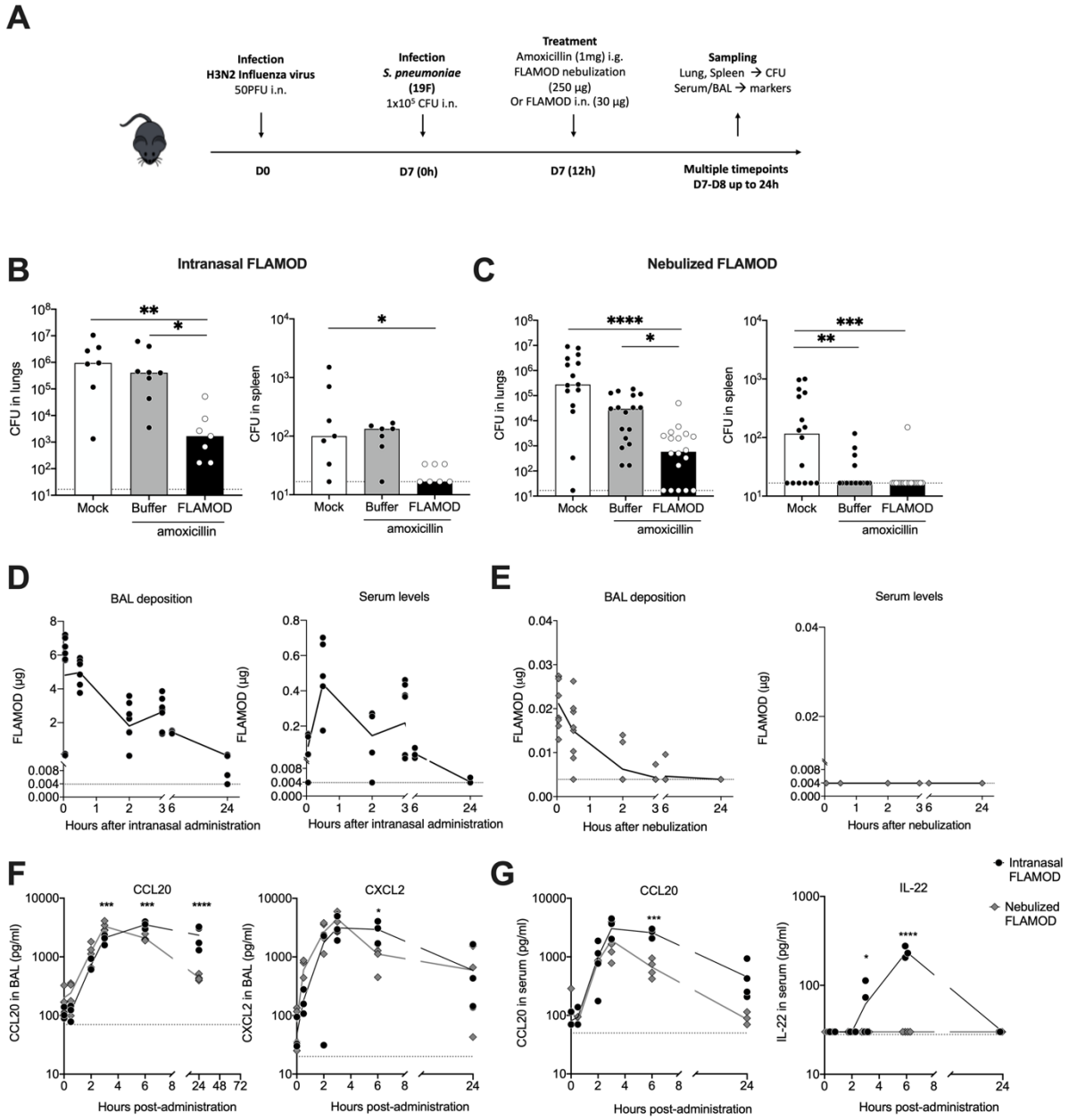

Figure 6. FLAMOD inhalation efficacy, kinetics and therapeutic activity in pneumococcal superinfection. (A) C57BL/6 mice (n=7-8 for intranasal and 15-19 for nebulization, per condition) were infected intranasally with influenza virus followed 7 days later by intranasal inoculation of $1x10^5$ CFU of *S. pneumoniae* 19F. Animals were treated at 12 hours post pneumococcal infection by intranasal administration of 2.5 µg **(B, F-G) or** 30 µg **(D)** FLAMOD or nebulization with 1 ml of FLAMOD at 250 µg/ml in NaPi buffer **(C, E-G)** combined with intragastric administration of 1 mg amoxicillin. Mock animals received

447 NaPi buffer and water. **(B-C)** Lungs and spleen for CFU were sampled 12 h post-treatment to
448 monitor therapeutic effects of intranasal administration **(B)** or nebulized FLAMOD **(C)**.
449 Statistical differences between the groups were analyzed by One-way ANOVA (*$p<0.05$,
450 **$p<0.01$, ***$p<0.001$, ****$p<0.0001$). **(D-G)** BAL and serum were sampled to measure
451 FLAMOD and immune activity. **(D-E)** FLAMOD distribution in BAL and serum after
452 intranasal administration **(D)** and nebulized FLAMOD **(E)**. FLAMOD was measured by
453 ELISA. LLOQ was fixed to 4 ng/ml. **(F-G)** Cytokine and chemokine production in BAL **(F)**
454 and serum **(G)** in response to FLAMOD inhalation methods. Statistical differences between
455 the two methods over time were analyzed using two-way ANOVA (*$p<0.05$, **$p<0.01$,
456 ***$p<0.001$, ****$p<0.0001$).
457

458 **4. Discussion**

459 This study underscores the potent immunostimulatory effects of nebulized flagellin
460 (FLAMOD) on the respiratory tract's immune defenses by combining quantitative analysis of
461 the biologic and the immune responses to it in the airways and bloodstream, as well as its
462 therapeutic efficacy. Although FLAMOD has been administered intranasally to target the lower
463 respiratory tract in mice, this route is not appropriate for similar targeting in humans. To
464 overcome this limitation and bridge the translational gap for this therapeutic, we engineered a
465 new custom-designed chamber integrated with the Aerogen Solo® vibrating mesh nebulizer.
466 Despite observing low lung deposition of nebulized FLAMOD, our results indicate that the
467 immunomodulatory and therapeutic efficacy of FLAMOD remained potent. Remarkably, our
468 aerosol delivery system achieved comparable therapeutic outcomes to intranasal administration
469 against pneumococcal pneumonia [15, 16], despite delivering doses 5-to-300-fold lower, as
470 defined by scintigraphy and ELISA data, respectively. Furthermore, nebulization was not
471 linked to any significant systemic exposure at the deposited dose achieved, thereby
472 highlighting both the relevance of the delivery methodology and the safety profile. Our findings
473 provide robust evidence supporting the development of FLAMOD as an immune-booster
474 complementing antibiotic therapy against respiratory bacterial pathogens with high potency
475 even at low concentrations.

476 Scintigraphy analysis unveils distinct contrast in deposition patterns between nebulized and
477 intranasally administered FLAMOD. A small fraction, less than 1%, of the nebulized
478 formulation is found to reach the lower airways, contrasting sharply with the intranasal route,
479 which achieves a deposition exceeding 40%. Furthermore, scintigraphy demonstrates
480 pronounced divergence in distribution across respiratory compartments between nebulized and
481 intranasal routes. Notably, the intranasal approach exhibits heightened exposure of the trachea,
482 whereas such exposure is lacking in the nebulization method. Despite these differences in

483 deposition patterns, RNAseq analysis indicates activation of similar immune pathways in the
484 lungs across both administration approaches. Moreover, RT-qPCR analysis of genes encoding
485 immune mediators reveals comparable or even elevated levels of transcriptional activation in
486 the nasal compartment, trachea, and bronchial epithelium following nebulization, in contrast
487 to intranasal administration. These findings suggest that saturation of immune activation is
488 achieved at low doses of FLAMOD effect. While it has been previously inferred that inhalation
489 of flagellin does not enter the bloodstream [11], this study was the first to measure FLAMOD
490 using a new ELISA test developed for this purpose. Compared to scintigraphy, ELISA
491 measurements reported much lower levels in the deposition of FLAMOD in the pulmonary
492 compartment shortly after administration: less than 0.1% for nebulized FLAMOD versus 30%
493 for intranasal administration. These findings strongly suggest rapid elimination of nebulized
494 FLAMOD within the airways, despite the differential deposition detection by the two
495 quantification methods used.
496 Several factors could contribute to accelerated FLAMOD elimination upon nebulization. The
497 intranasal administration facilitates the entry of the biologic solution into the airways primarily
498 though gravitational forces and diffusion mechanisms. In contrast, nebulization generates fine
499 liquid particles that deeply penetrate tissues via the respiratory flow [42]. The interaction of
500 nebulized particles with various components such as epithelial lining fluid factors, mucus,
501 pulmonary surfactants, epithelial cells and alveolar macrophages is expected to be of a specific
502 nature. Consequently, these distinct inhalation methods lead to differing spatial distributions
503 and interactions within the respiratory system, which may play a crucial role in the observed
504 degradation dynamics of FLAMOD. Previous studies have reported that proteins deposited in
505 the airways by nebulization can be eliminated by various mechanisms including pulmonary
506 surfactant opsonization [43], endocytosis or phagocytosis by alveolar macrophages [44]
507 proteolytic degradation, mucus entrapping, or mucociliary clearance [45]. It is usually

508 considered that mucus is not a barrier for proteins <500 kDa while particles trapped in the
509 mucus, can be transported to the pharynx by the mucociliary clearance mechanisms [45, 46].
510 The conducting airways including bronchi and alveoli contain many secreted and cell-
511 associated proteases such cathepsins, dipeptidylpeptidases, metalloproteinases,
512 carboxypeptidases, or xenobiotic metabolizing enzymes such as cytochromes that can be active
513 against biologics [47, 48]. Of note, FLAMOD is derived from the native *Salmonella* flagellin
514 that is known to contain multiple proteolytic cleavage sites in the distal region, rendering
515 FLAMOD prone to degradation by proteases [49]. Whether nebulization exacerbates these
516 catabolic processes compared to intranasal delivery remains to be determined.
517 Biologic drugs specific for treating lung conditions, such as the recombinant human DNAse
518 used as a mucolytic in cystic fibrosis lung disease, have been adapted for nebulization as it is
519 a unique method to compartmentalize the drug activity within the respiratory tract, thereby
520 mitigating systemic exposure and potential toxicity [50, 51]. While the TLR5-dependent
521 immunomodulation in the airways presents a promising therapeutic avenue, it is important to
522 acknowledge a potential caveat stemming from systemic exposure. TLR5, being widely
523 expressed across various cells and tissues, carries the risk of precipitating undesired
524 inflammation, commonly referred to as immune-related adverse events [52]. Nebulization is
525 thus an attractive administration route for our biologic in order to mitigate such events. To
526 assess systemic exposure to FLAMOD, the production of serum IL-22 serves as a surrogate
527 marker. Previous studies have established that IL-22 necessitates flagellin-mediated activation
528 of TLR5 signaling in dendritic cells derived from either blood or tissue parenchyma [11, 38,
529 39]. This study showed no or very low levels of serum IL-22 after inhalation, corroborating the
530 FLAMOD dosing in serum and insinuating little to no systemic leakage. The efficient
531 elimination of nebulized FLAMOD may contribute to the minimal systemic exposure
532 observed. Factors that influence systemic absorption include properties of the aerosol particles

533 such as pH, charge, and surface activity. Studies have indicated a variable availability of
534 inhaled proteins in the bloodstream, ranging from 10% to 50% [53]. In mice, systemic exposure
535 to antibodies via orotracheal inhalation is notably low, despite efficient deposition in the
536 airways [54]. This trend is echoed in clinical trials, where nebulized administration of
537 antibodies results in systemic exposure of approximately 1% of the deposited dose [55].
538 Despite the rapid clearance of FLAMOD, its administration via nebulization still effectively
539 stimulates innate immunity within the lungs, mirroring the response observed with the
540 intranasal route. TLR signaling, including activation of TLR5, initiates immediate NF-κB
541 activation within minutes, alongside the induction of negative feedback mechanisms [8, 9].
542 This "hit and run" activation of TLR5 rationalizes the efficacy of nebulized FLAMOD despite
543 its short residency half-life within respiratory tissues. Although nebulized FLAMOD induces
544 a transient immunomodulatory effect on neutrophil mobilization in alveoli and bronchi, it
545 promotes a more rapid resolution of the TLR5-mediated pro-inflammatory response compared
546 to intranasal delivery. This accelerated resolution aligns with the observed differences in the
547 biodistribution of intranasal versus nebulized FLAMOD, with intranasal FLAMOD persisting
548 longer in the lungs compared to the nebulized form. However, the precise mechanisms
549 underlying these differential kinetics require further investigation.
550 The effectiveness of nebulized FLAMOD as an adjunct to antibiotics was demonstrated in two
551 clinically relevant models of pneumonia: primary pneumonia and pneumococcal
552 superinfection, which occurs when there is a pre-existing influenza virus infection.
553 Furthermore, this proof-of-concept was confirmed using two different serotypes of
554 pneumococcus, one susceptible and the other resistant to amoxicillin (with MIC_{AMX} values of
555 0.016 μg/ml and 1.5 μg/ml respectively). The results from this study align with the clinical
556 development of nebulized FLAMOD and support previous findings from intranasal
557 administration in pneumonia treatment [15, 16]. Analysis of FLAMOD distribution throughout

558 the body, as well as the immune responses in the lungs and blood following inhalation, revealed
559 that pneumonia-induced damage had minimal impact on the observed bioavailability and
560 immune activation patterns. This reinforces the safety and effectiveness of our therapeutic
561 approach targeting the respiratory tissues.
562 In conclusion, our findings underscore the intricate interplay between inhalation methods,
563 respiratory and systemic distribution, and immunomodulatory activity of FLAMOD, which are
564 critical considerations in optimizing therapeutic outcomes and minimizing adverse effects. It
565 will be important to extend these investigations to the study of more representative models to
566 allow better translation of nebulized FLAMOD to the clinic. More appropriate species, for
567 better defining nebulized FLAMOD PK and PD parameters with higher translational value,
568 will include pig models and non-human primate models. Nevertheless, this study has
569 determined nebulization as an effective and safe method for next step development of host-
570 directed lung-targeting therapies of pneumonia.
571

572 **Conflicts of interest**

573 JCS, CCa and NHV are inventors of the patents WO2009156405, WO2011161491,
574 WO2015011254, and WO2016102536 that describe the use of flagellin as biologic against
575 infectious diseases and the patent WO2023275292 on the formulation of FLMAOD. NHV is a
576 cofounder of Cynbiose Respiratory and does not hold stock options. In the last few years, she
577 has been paid as a scientific advisor (Novartis, European Commission, Immune Biosolution,
578 ANR, Alvea/Telis Bioscience). Her group has financial relationships with private-sector
579 entities (Nemera, Aptar Pharma, Affilogic, 4P-Pharma, EuroAPI) outside the scope of the
580 present work and Aerogen within the scope of this study. RMACL is named inventor on several
581 vibrating mesh nebulizer patents. Authors declare no other competing interests.

582

583 **Author Contributions**

584 MB, CCo, JP planned studies, performed experiments and analyzed data. DC, DS performed
585 experiments. YZ analyzed transcriptomic data. RM provided the nebulizers plus controllers
586 and reviewed the paper. FW provided the clinical isolate LILPNEUHC 19F strain and
587 reviewed the paper. MB, CCo, YZ, JCS and CCa wrote the paper with input from all authors.
588 MB, JCS, CCa and NHV supervised the project.

589

590 **Funding.** The study was funded by INSERM, Institut Pasteur de Lille, Université de Lille, the
591 project FAIR that received funding from the European Union's Horizon 2020 research and
592 innovation program under grant agreement No 847786, and the Agence Nationale de la
593 Recherche (grant ANR-19-CE18- 0030-01).

594

Acknowledgements. We thank the Vaccine Development department of Statens Serum Institut (Denmark) for the manufacture and supply of FLAMOD. We thank the PLETHA animal facility from UMS2014-US41-PLBS.

599 **References**

600

601 [1] https://www.who.int/news/item/09-12-2020-who-reveals-leading-causes-of-death-and-
602 disability-worldwide-2000-2019, (2019).
603 [2] C. Scelfo, F. Menzella, M. Fontana, G. Ghidoni, C. Galeone, N.C. Facciolongo, Pneumonia
604 and Invasive Pneumococcal Diseases: The Role of Pneumococcal Conjugate Vaccine in the
605 Era of Multi-Drug Resistance, Vaccines (Basel), 9 (2021).
606 [3] L.M. Wang, T. Cravo Oliveira Hashiguchi, M. Cecchini, Impact of vaccination on carriage
607 of and infection by antibiotic-resistant bacteria: a systematic review and meta-analysis, Clin
608 Exp Vaccine Res, 10 (2021) 81-92.
609 [4] A. Lochen, N.J. Croucher, R.M. Anderson, Divergent serotype replacement trends and
610 increasing diversity in pneumococcal disease in high income settings reduce the benefit of
611 expanding vaccine valency, Sci Rep, 10 (2020) 18977.
612 [5] J. Liñares, C. Ardanuy, R. Pallares, A. Fenoll, Changes in antimicrobial resistance,
613 serotypes and genotypes in Streptococcus pneumoniae over a 30-year period, Clin Microbiol
614 Infect, 16 (2010) 402-410.
615 [6] M. Miethke, M. Pieroni, T. Weber, M. Brönstrup, P. Hammann, L. Halby, P.B. Arimondo,
616 P. Glaser, B. Aigle, H.B. Bode, R. Moreira, Y. Li, A. Luzhetskyy, M.H. Medema, J.-L.
617 Pernodet, M. Stadler, J.R. Tormo, O. Genilloud, A.W. Truman, K.J. Weissman, E. Takano, S.
618 Sabatini, E. Stegmann, H. Brötz-Oesterhelt, W. Wohlleben, M. Seemann, M. Empting, A.K.H.
619 Hirsch, B. Loretz, C.-M. Lehr, A. Titz, J. Herrmann, T. Jaeger, S. Alt, T. Hesterkamp, M.
620 Winterhalter, A. Schiefer, K. Pfarr, A. Hoerauf, H. Graz, M. Graz, M. Lindvall, S. Ramurthy,
621 A. Karlén, M. van Dongen, H. Petkovic, A. Keller, F. Peyrane, S. Donadio, L. Fraisse, L.J.V.
622 Piddock, I.H. Gilbert, H.E. Moser, R. Müller, Towards the sustainable discovery and
623 development of new antibiotics, Nature Reviews Chemistry, 5 (2021) 726-749.

624 [7] R.S. Wallis, A. O'Garra, A. Sher, A. Wack, Host-directed immunotherapy of viral and
625 bacterial infections: past, present and future, Nat Rev Immunol, 23 (2023) 121-133.
626 [8] K.A. Fitzgerald, J.C. Kagan, Toll-like Receptors and the Control of Immunity, Cell, 180
627 (2020) 1044-1066.
628 [9] J. Yang, H. Yan, TLR5: beyond the recognition of flagellin, Cellular & Molecular
629 Immunology, 14 (2017) 1017-1019.
630 [10] L. Janot, J.C. Sirard, T. Secher, N. Noulin, L. Fick, S. Akira, S. Uematsu, A. Didierlaurent,
631 T. Hussell, B. Ryffel, F. Erard, Radioresistant cells expressing TLR5 control the respiratory
632 epithelium's innate immune responses to flagellin, Eur J Immunol, 39 (2009) 1587-1596.
633 [11] L. Van Maele, D. Fougeron, L. Janot, A. Didierlaurent, D. Cayet, J. Tabareau, M. Rumbo,
634 S. Corvo-Chamaillard, S. Boulenouar, S. Jeffs, L. Vande Walle, M. Lamkanfi, Y. Lemoine, F.
635 Erard, D. Hot, T. Hussell, B. Ryffel, A.G. Benecke, J.C. Sirard, Airway structural cells regulate
636 TLR5-mediated mucosal adjuvant activity, Mucosal Immunology, 7 (2014) 489-500.
637 [12] N. Muñoz, L. Van Maele, J.M. Marqués, A. Rial, J.C. Sirard, J.A. Chabalgoity, Mucosal
638 administration of flagellin protects mice from Streptococcus pneumoniae lung infection, Infect
639 Immun, 78 (2010) 4226-4233.
640 [13] A.K. Zgair, Flagellin administration protects respiratory tract from Burkholderia cepacia
641 infection, J Microbiol Biotechnol, 22 (2012) 907-916.
642 [14] F.S. Yu, M.D. Cornicelli, M.A. Kovach, M.W. Newstead, X. Zeng, A. Kumar, N. Gao,
643 S.G. Yoon, R.L. Gallo, T.J. Standiford, Flagellin stimulates protective lung mucosal immunity:
644 role of cathelicidin-related antimicrobial peptide, J Immunol, 185 (2010) 1142-1149.
645 [15] L. Matarazzo, F. Casilag, R. Porte, F. Wallet, D. Cayet, C. Faveeuw, C. Carnoy, J.C.
646 Sirard, Therapeutic Synergy Between Antibiotics and Pulmonary Toll-Like Receptor 5
647 Stimulation in Antibiotic-Sensitive or -Resistant Pneumonia, Front Immunol, 10 (2019) 723.

648 [16] R. Porte, D. Fougeron, N. Muñoz-Wolf, J. Tabareau, A.F. Georgel, F. Wallet, C. Paget,
649 F. Trottein, J.A. Chabalgoity, C. Carnoy, J.C. Sirard, A Toll-Like Receptor 5 Agonist Improves
650 the Efficacy of Antibiotics in Treatment of Primary and Influenza Virus-Associated
651 Pneumococcal Mouse Infections, Antimicrob Agents Chemother, 59 (2015) 6064-6072.
652 [17] C. Costa, J.C. Sirard, P.S. Gibson, J.W. Veening, E. Gjini, M. Baldry, Triggering Toll-
653 Like Receptor 5 signaling during pneumococcal superinfection prevents the selection of
654 antibiotic resistance, J Infect Dis, (2024).
655 [18] D.L. Goldblatt, J.R. Flores, G. Valverde Ha, A.M. Jaramillo, S. Tkachman, C.T.
656 Kirkpatrick, S. Wali, B. Hernandez, D.E. Ost, B.L. Scott, J. Chen, S.E. Evans, M.J. Tuvim,
657 B.F. Dickey, Inducible epithelial resistance against acute Sendai virus infection prevents
658 chronic asthma-like lung disease in mice, Br J Pharmacol, 177 (2020) 2256-2273.
659 [19] M.J. Tuvim, B.E. Gilbert, B.F. Dickey, S.E. Evans, Synergistic TLR2/6 and TLR9
660 activation protects mice against lethal influenza pneumonia, PLoS One, 7 (2012) e30596.
661 [20] J.M. Duggan, D. You, J.O. Cleaver, D.T. Larson, R.J. Garza, F.A. Guzmán Pruneda, M.J.
662 Tuvim, J. Zhang, B.F. Dickey, S.E. Evans, Synergistic interactions of TLR2/6 and TLR9
663 induce a high level of resistance to lung infection in mice, J Immunol, 186 (2011) 5916-5926.
664 [21] A. Iwasaki, E.F. Foxman, R.D. Molony, Early local immune defences in the respiratory
665 tract, Nat Rev Immunol, 17 (2017) 7-20.
666 [22] W.R. Ke, R.Y.K. Chang, H.K. Chan, Engineering the right formulation for enhanced drug
667 delivery, Adv Drug Deliv Rev, 191 (2022) 114561.
668 [23] R. MacLoughlin, I. Martin-Loeches, Not all nebulizers are created equal: Considerations
669 in choosing a nebulizer for aerosol delivery during mechanical ventilation, Expert Rev Respir
670 Med, 17 (2023) 131-142.

671 [24] E. Bodier-Montagutelli, A. Mayor, L. Vecellio, R. Respaud, N. Heuze-Vourc'h, Designing
672 inhaled protein therapeutics for topical lung delivery: what are the next steps?, Expert Opin
673 Drug Deliv, 15 (2018) 729-736.
674 [25] T.C. Carvalho, J.T. McConville, The function and performance of aqueous aerosol devices
675 for inhalation therapy, J Pharm Pharmacol, 68 (2016) 556-578.
676 [26] S.P. Hertel, G. Winter, W. Friess, Protein stability in pulmonary drug delivery via
677 nebulization, Adv Drug Deliv Rev, 93 (2015) 79-94.
678 [27] L.-A. Keller, O. Merkel, A. Popp, Intranasal drug delivery: opportunities and toxicologic
679 challenges during drug development, Drug Delivery and Translational Research, 12 (2022)
680 735-757.
681 [28] S. Ehrmann, Vibrating Mesh Nebulizers-Can greater drug delivery to the airways and
682 lungs improve respiratory outcomes?, European Respiratory & Pulmonary Diseases, 4 (2018)
683 33-43.
684 [29] W. Longest, B. Spence, M. Hindle, Devices for Improved Delivery of Nebulized
685 Pharmaceutical Aerosols to the Lungs, J Aerosol Med Pulm Drug Deliv, 32 (2019) 317-339.
686 [30] J.N. Pritchard, R.H. Hatley, J. Denyer, D.V. Hollen, Mesh nebulizers have become the
687 first choice for new nebulized pharmaceutical drug developments, Ther Deliv, 9 (2018) 121-
688 136.
689 [31] L. Sweeney, A.P. McCloskey, G. Higgins, J.M. Ramsey, S.-A. Cryan, R. MacLoughlin,
690 Effective nebulization of interferon-γ using a novel vibrating mesh, Respiratory Research, 20
691 (2019) 66.
692 [32] C. Nempont, D. Cayet, M. Rumbo, C. Bompard, V. Villeret, J.C. Sirard, Deletion of
693 flagellin's hypervariable region abrogates antibody-mediated neutralization and systemic
694 activation of TLR5-dependent immunity, J Immunol, 181 (2008) 2036-2043.

695 [33] C. Paget, S. Ivanov, J. Fontaine, F. Blanc, M. Pichavant, J. Renneson, E. Bialecki, J.
696 Pothlichet, C. Vendeville, G. Barba-Spaeth, M.R. Huerre, C. Faveeuw, M. Si-Tahar, F.
697 Trottein, Potential role of invariant NKT cells in the control of pulmonary inflammation and
698 CD8+ T cell response during acute influenza A virus H3N2 pneumonia, J Immunol, 186 (2011)
699 5590-5602.
700 [34] Y. Hiriart, M. Serradell, A. Martinez, S. Sampaolesi, D.G. Maciel, J.A. Chabalgoity, L.
701 Yim, G. Algorta, M. Rumbo, Generation and selection of anti-flagellin monoclonal antibodies
702 useful for serotyping Salmonella enterica, Springerplus, 2 (2013) 640.
703 [35] K. Chen, T. Eddens, G. Trevejo-Nunez, E.E. Way, W. Elsegeiny, D.M. Ricks, A.V. Garg,
704 C.J. Erb, M. Bo, T. Wang, W. Chen, J.S. Lee, S.L. Gaffen, J.K. Kolls, IL-17 Receptor Signaling
705 in the Lung Epithelium Is Required for Mucosal Chemokine Gradients and Pulmonary Host
706 Defense against K. pneumoniae, Cell Host Microbe, 20 (2016) 596-605.
707 [36] M.I. Love, W. Huber, S. Anders, Moderated estimation of fold change and dispersion for
708 RNA-seq data with DESeq2, Genome Biology, 15 (2014) 550.
709 [37] D. Fougeron, L. Van Maele, P. Songhet, D. Cayet, D. Hot, N. Van Rooijen, H.J.
710 Mollenkopf, W.D. Hardt, A.G. Benecke, J.C. Sirard, Indirect Toll-like receptor 5-mediated
711 activation of conventional dendritic cells promotes the mucosal adjuvant activity of flagellin
712 in the respiratory tract, Vaccine, 33 (2015) 3331-3341.
713 [38] M.A. Kinnebrew, C.G. Buffie, G.E. Diehl, L.A. Zenewicz, I. Leiner, T.M. Hohl, R.A.
714 Flavell, D.R. Littman, E.G. Pamer, Interleukin 23 production by intestinal CD103(+)CD11b(+)
715 dendritic cells in response to bacterial flagellin enhances mucosal innate immune defense,
716 Immunity, 36 (2012) 276-287.
717 [39] L. Van Maele, C. Carnoy, D. Cayet, P. Songhet, L. Dumoutier, I. Ferrero, L. Janot, F.
718 Erard, J. Bertout, H. Leger, F. Sebbane, A. Benecke, J.C. Renauld, W.D. Hardt, B. Ryffel, J.C.

719 Sirard, TLR5 signaling stimulates the innate production of IL-17 and IL-22 by
720 CD3(neg)CD127+ immune cells in spleen and mucosa, J Immunol, 185 (2010) 1177-1185.
721 [40] L.R. Prince, M.K. Whyte, I. Sabroe, L.C. Parker, The role of TLRs in neutrophil
722 activation, Current Opinion in Pharmacology, 11 (2011) 397-403.
723 [41] T.R. Hawn, W.R. Berrington, I.A. Smith, S. Uematsu, S. Akira, A. Aderem, K.D. Smith,
724 S.J. Skerrett, Altered inflammatory responses in TLR5-deficient mice infected with Legionella
725 pneumophila, J Immunol, 179 (2007) 6981-6987.
726 [42] S. Ehrmann, O. Schmid, C. Darquenne, B. Rothen-Rutishauser, J. Sznitman, L. Yang, H.
727 Barosova, L. Vecellio, J. Mitchell, N. Heuze-Vourc'h, Innovative preclinical models for
728 pulmonary drug delivery research, Expert Opin Drug Deliv, 17 (2020) 463-478.
729 [43] T. Tschernig, N.T. Veith, E. Diler, M. Bischoff, C. Meier, M. Schicht, The importance of
730 surfactant proteins—New aspects on macrophage phagocytosis, Annals of Anatomy -
731 Anatomischer Anzeiger, 208 (2016) 142-145.
732 [44] C. Lombry, D.A. Edwards, V. Preat, R. Vanbever, Alveolar macrophages are a primary
733 barrier to pulmonary absorption of macromolecules, Am J Physiol Lung Cell Mol Physiol, 286
734 (2004) L1002-1008.
735 [45] E. Frohlich, S. Salar-Behzadi, Oral inhalation for delivery of proteins and peptides to the
736 lungs, Eur J Pharm Biopharm, 163 (2021) 198-211.
737 [46] S.S. Olmsted, J.L. Padgett, A.I. Yudin, K.J. Whaley, T.R. Moench, R.A. Cone, Diffusion
738 of macromolecules and virus-like particles in human cervical mucus, Biophys J, 81 (2001)
739 1930-1937.
740 [47] Z. Enlo-Scott, E. Bäckström, I. Mudway, B. Forbes, Drug metabolism in the lungs:
741 opportunities for optimising inhaled medicines, Expert Opinion on Drug Metabolism &
742 Toxicology, 17 (2021) 611-625.

743 [48] F. Oesch, E. Fabian, R. Landsiedel, Xenobiotica-metabolizing enzymes in the lung of
744 experimental animals, man and in human lung models, Archives of Toxicology, 93 (2019)
745 3419-3489.
746 [49] F. Vonderviszt, S. Aizawa, K. Namba, Role of the disordered terminal regions of flagellin
747 in filament formation and stability, J Mol Biol, 221 (1991) 1461-1474.
748 [50] J.S. Tepper, P.J. Kuehl, S. Cracknell, K.J. Nikula, L. Pei, J.D. Blanchard, Symposium
749 Summary: "Breathe In, Breathe Out, Its Easy: What You Need to Know About Developing
750 Inhaled Drugs", Int J Toxicol, 35 (2016) 376-392.
751 [51] S. Mahri, T. Wilms, P. Hagedorm, M.-J. Guichard, K. Vanvarenberg, M. Dumoulin, H.
752 Frijlink, R. Vanbever, Nebulization of PEGylated recombinant human deoxyribonuclease I
753 using vibrating membrane nebulizers: A technical feasibility study, European Journal of
754 Pharmaceutical Sciences, 189 (2023) 106522.
755 [52] M. Conroy, J. Naidoo, Immune-related adverse events and the balancing act of
756 immunotherapy, Nature Communications, 13 (2022) 392.
757 [53] R. Siekmeier, G. Scheuch, Systemic treatment by inhalation of macromolecules--
758 principles, problems, and examples, J Physiol Pharmacol, 59 Suppl 6 (2008) 53-79.
759 [54] T. Secher, E. Dalonneau, M. Ferreira, C. Parent, N. Azzopardi, G. Paintaud, M. Si-Tahar,
760 N. Heuze-Vourc'h, In a murine model of acute lung infection, airway administration of a
761 therapeutic antibody confers greater protection than parenteral administration, J Control
762 Release, 303 (2019) 24-33.
763 [55] A. Proudfoot, A. Bayliffe, C.M. O'Kane, T. Wright, A. Serone, P.J. Bareille, V. Brown,
764 U.I. Hamid, Y. Chen, R. Wilson, J. Cordy, P. Morley, R. de Wildt, S. Elborn, M. Hind, E.R.
765 Chilvers, M. Griffiths, C. Summers, D.F. McAuley, Novel anti-tumour necrosis factor
766 receptor-1 (TNFR1) domain antibody prevents pulmonary inflammation in experimental acute
767 lung injury, Thorax, 73 (2018) 723-730.

768

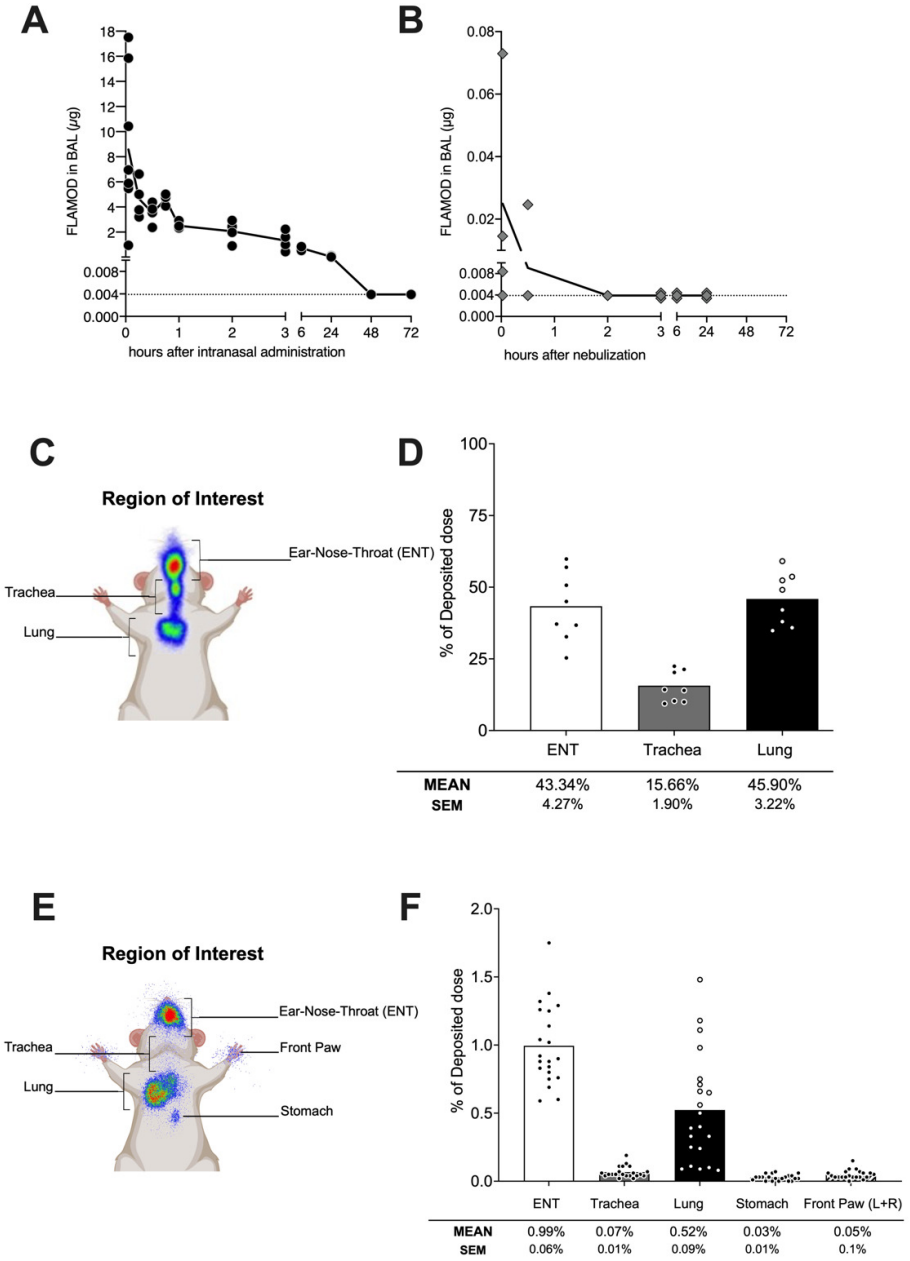

Figure 1. FLAMOD biodistribution after intranasal or aerosol inhalation.

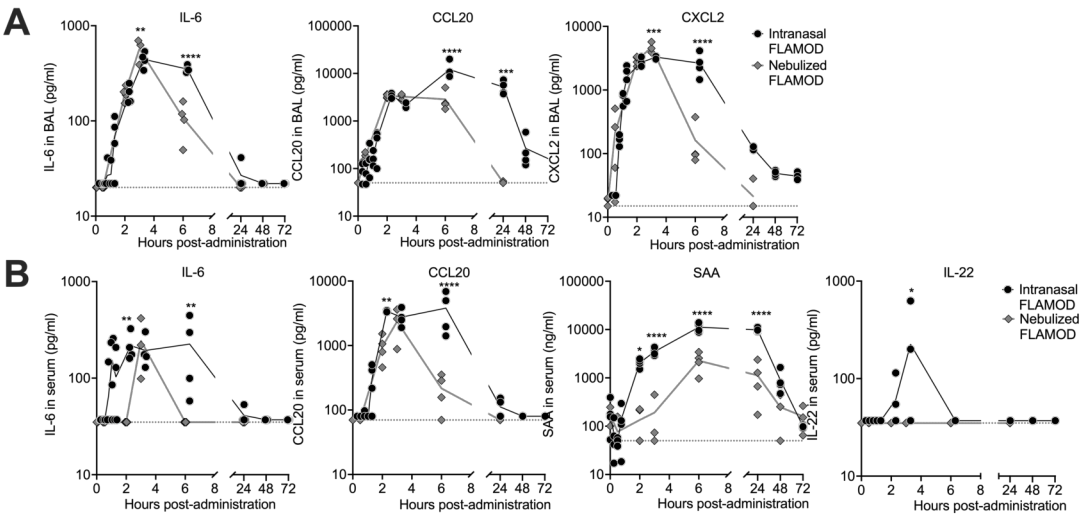

Figure 2. Transient innate immune activation following FLAMOD inhalation.

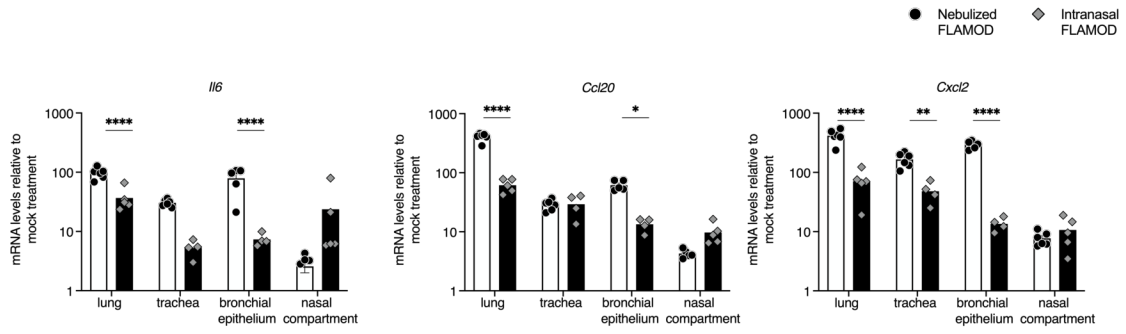

Figure 3. Compartmentalization of transcriptional response to FLAMOD inhalation.

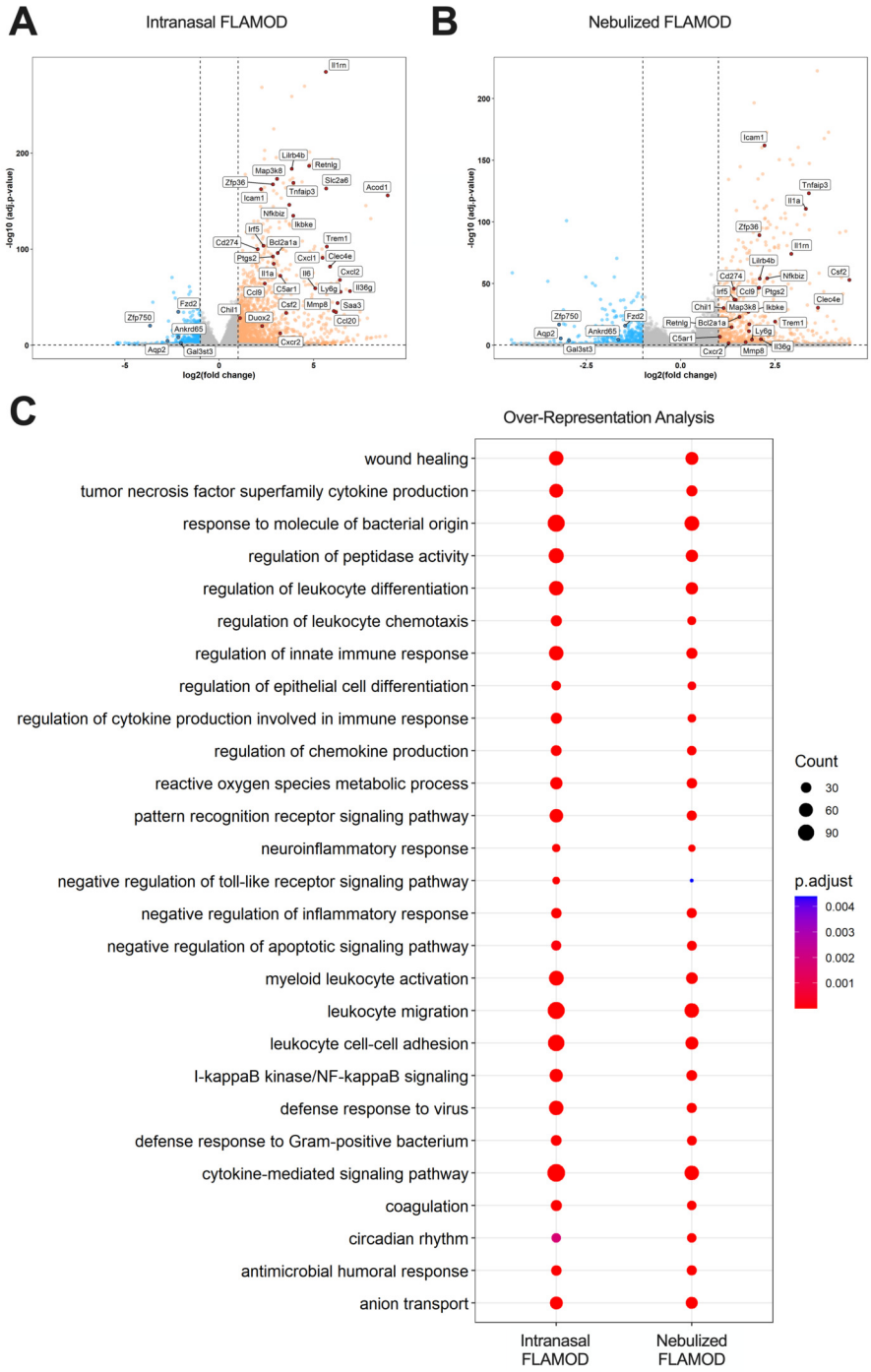

Figure 4. FLAMOD inhalation by the intranasal or nebulization route activates similar innate immune responses.

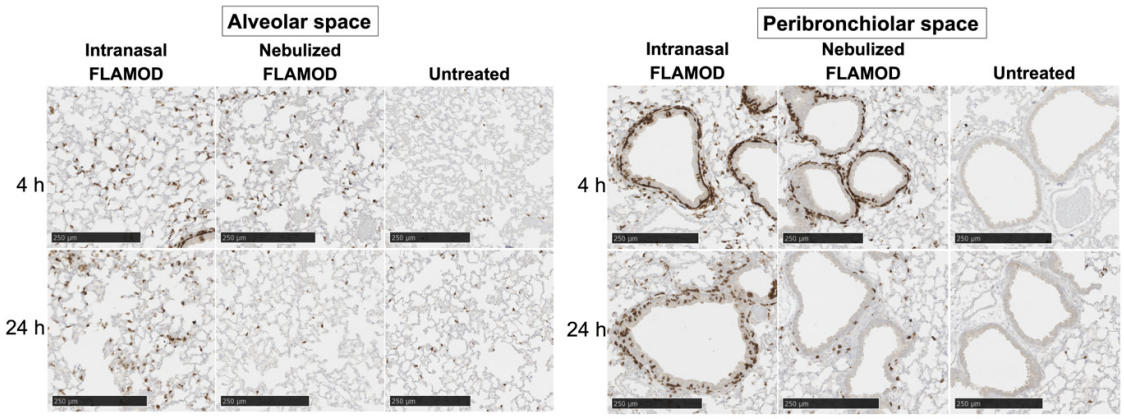

Figure 5. Transient neutrophil recruitment in response to FLAMOD inhalation.

Figure 6

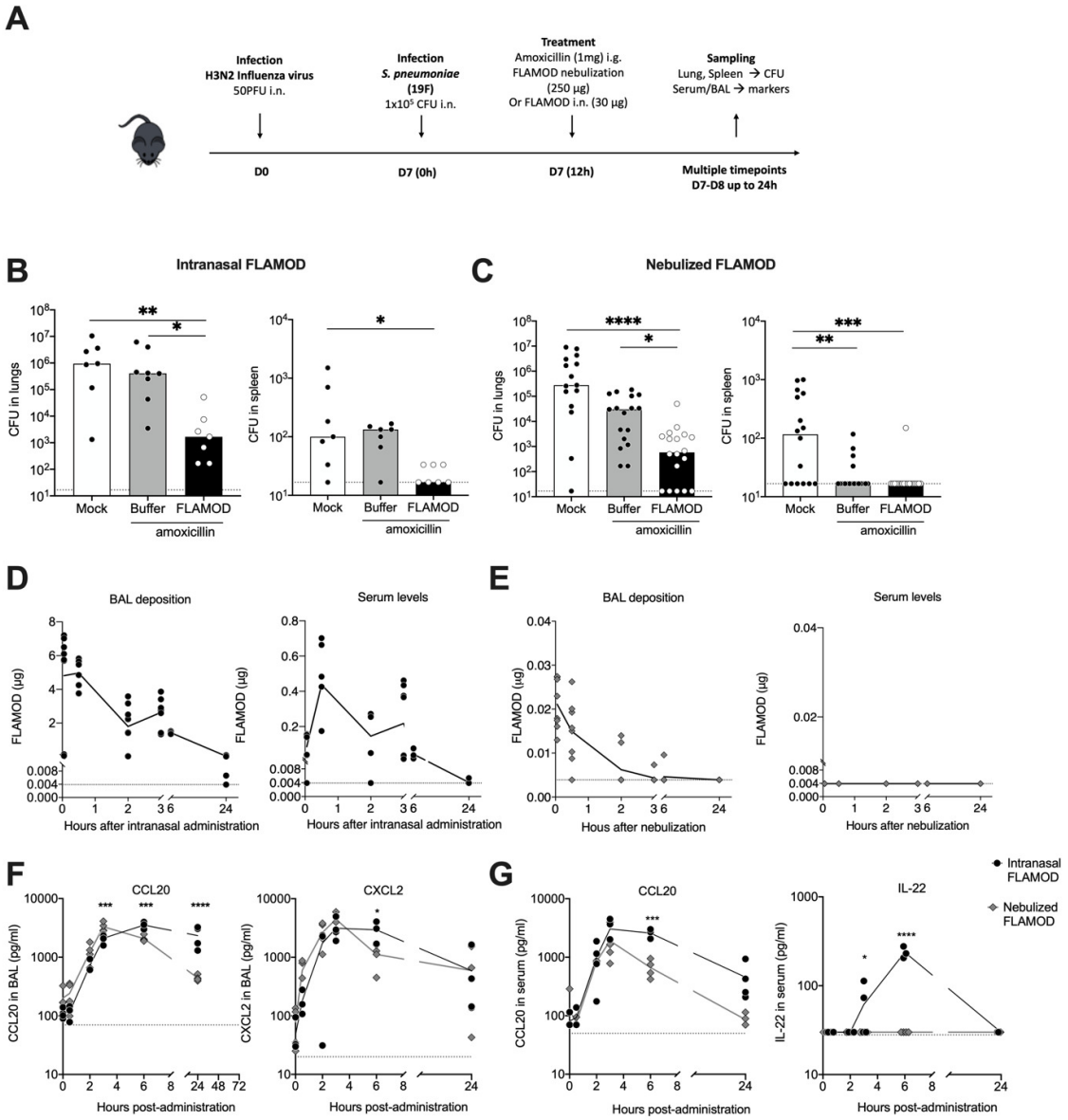

Figure 6. FLAMOD inhalation efficacy, kinetics and therapeutic activity in pneumococcal superinfection.